Thermodynamic Investigation of SNG Production Based on Dual Fluidized Bed Gasification of Biogenic Residues

A. Bartik[1*], F. Benedikt[1], A. Lunzer[2], C. Walcher[2], S. Müller[2], H. Hofbauer[1]

1. TU Wien, Institute of Chemical, Environmental and Bioscience Engineering, Getreidemarkt 9/166, 1060 Vienna, Austria
2. Energy & Chemical Engineering GmbH, Pappelstraße 13, 1140 Vienna, Austria

*corresponding author, alexander.bartik@tuwien.ac.at

Abstract

Natural gas is an important commodity in the European energy market. A promising concept for the production of synthetic natural gas on a carbon neutral basis is presented by the gasification of biogenic residues and the further reaction to a methane-rich gas. This paper investigates the thermodynamics of methanation for different product gas compositions of the dual fluidized bed gasification technology. A complete methanation of the carbon oxides is possible by the utilization of a product gas from the sorption enhanced reforming process. For product gases from conventional or carbon dioxide gasification, only partial methanation of carbon monoxide occurs. Additionally, proper handling of carbon depositions through adjustments of feed gas composition and operational parameters in the methanation reactor are essential. Temperature and pressure variations allow a thermodynamically optimized operation, which can reduce energy costs for compression or lower the amount of gas upgrading for grid feed-in. Vice versa, it is shown that the feed gas can be optimally adjusted to the operational parameters of the methanation via the sorption enhanced reforming process.

1. Introduction

Increasing greenhouse gas emissions and the limited availability of primary energy carriers directed the energy policy of the European Union towards sustainable and innovative energy technologies [1]. Natural gas is one of the most important primary energy carriers in Europe, but its availability is heavily dependent on the non-European market. The production of synthetic natural gas (SNG) from biogenic residues offers a promising alternative to the utilization of fossil fuels and represents a novel concept to support the current energy strategy of the European Union [1, 2].

One possible process route is the dual fluidized bed (DFB) gasification, which allows the utilization of locally available residual biogenic or waste resources and offers possibilities for the production of highly valuable secondary energy carriers on a carbon neutral basis [3, 4]. In combination with sorption enhanced reforming (SER) this technology enables the production of a nitrogen-free product gas with adjustable hydrogen to carbon monoxide and hydrogen to carbon dioxide contents [5].

Before the product gas from the DFB process can be fed to the methanation unit, rigorous gas cleaning is required in order to protect the downstream equipment and the methanation catalyst [6-8].

For the methanation reactor itself, several concepts have been utilized. Adiabatic or cooled fixed bed reactors, fluidized bed reactors, three-phase reactors or micro-reactors. However, only adiabatic fixed bed methanation is commercially available as of today. This variety of reactor types

also explains the wide range of operation conditions. Temperatures from 250 °C to 700° C and pressures from 1 bar_a to 87 bar_a have been applied. From a thermodynamic point of view the methanation is favored at low temperatures and high pressures [9, 10].

In order to feed the generated gas into the Austrian gas grid, the feed-in regulations must be satisfied [11]. Alternatively, a mixture of CH_4 and H_2, also referred to as hythane, can be generated as a substitute for natural gas in industrial applications [12].

The main chemical species, which are involved in the methanation reaction system, are CH_4, H_2, CO, CO_2 and H_2O. The corresponding reaction equations are the CO-methanation,

$$CO + 3H_2 \rightleftharpoons CH_4 + H_2O \quad \Delta H_R^{300} = -216 \frac{kJ}{mol} \quad (1)$$

the reverse water gas shift reaction, and

$$CO_2 + H_2 \rightleftharpoons CO + H_2O \quad \Delta H_R^{300} = 39 \frac{kJ}{mol} \quad (2)$$

the CO_2-methanation (combination of (2) and (1)).

$$CO_2 + 4H_2 \rightleftharpoons CH_4 + 2H_2O \; \Delta H_R^{300} = -177 \frac{kJ}{mol} \quad (3)$$

Additionally, the reaction enthalpies at 300 °C (ΔH_R^{300}) are given. Besides these species, the product gas of the DFB gasifier also contains higher hydrocarbons. As the main component ethylene (C_2H_4) is identified and is thus included here [13]. The hydrogenation to methane can be written as:

$$C_2H_4 + 2H_2 \rightarrow 2CH_4 \quad \Delta H_R^{300} = -209 \frac{kJ}{mol} \quad (4)$$

A deactivation mechanism of the catalyst, which cannot be prevented by gas cleaning steps, is the formation of solid carbon on the catalyst. While adsorbed carbon on the catalyst surface is a necessary reaction intermediate during methanation, the formation of stable deposits leads to catalyst fouling [14]. Thermodynamically, this deposition can be accounted for by the Boudouard reaction.

$$2CO \rightleftharpoons CO_2 + C(s) \quad \Delta H_R^{300} = -174 \frac{kJ}{mol} \quad (5)$$

The deposited surface carbon can also be hydrogenated to methane,

$$C(s) + 2H_2 \rightleftharpoons CH_4 \quad \Delta H_R^{300} = -82.1 \frac{kJ}{mol} \quad (6)$$

or undergo gasification with steam [15].

$$C(s) + H_2O \rightleftharpoons CO + H_2 \quad \Delta H_R^{300} = 134 \frac{kJ}{mol} \quad (7)$$

These reactions show that increased amounts of H_2, H_2O or CO_2 in the product gas might prevent the carbon deposition.

A different form of deposition can occur through the adsorption of higher hydrocarbons like C_2H_4 on the catalyst surface. Between 500 and 600 °C, this can lead to coke deposits [16].

If kinetic models are considered, all of the above mentioned reaction pathways have to be taken into consideration. The catalytic methanation of syngas is, however, mostly limited by heat and mass transfer and not by kinetics [10]. For temperatures down to 320 °C the gas composition is close to the thermodynamic equilibrium [17, 18]. A thermodynamic calculation thus provides a good estimation of the expected gas composition. Because of the broad variety of possible carbon species, deviations from thermodynamic equilibrium for carbon deposition have to be expected [10]. Nevertheless, graphitic carbon has previously been used to elucidate this issue, since kinetic models are often only valid for specific reaction conditions and catalysts [19].

Extensive studies have been performed on the thermodynamics of methanation [14, 19, 20]. However, for systems with multiple simultaneous reactions, the effect of different product gas mixtures as well as temperature and pressure is not straightforward. Thus, the thermodynamic calculations in this paper are applied to

different product gas mixtures, which have been obtained by the gasification of different biogenic residues with the 100 kW_{th} DFB gasifier at TU Wien. The chosen feed gas compositions for the methanation aim at covering the broad range of product gas compositions, which can be produced by the DFB gasifier.

2. Concept and methodology

In order to calculate the thermodynamic equilibrium, only four of the seven reaction equations (Eq. (1) to Eq. (7)) need to be considered. Otherwise, the system would be overdetermined, because only four equations are linearly independent of each other. For example, the CO_2-methanation reaction can be seen as the reversed water gas shift reaction followed by the CO-methanation.

Thermodynamic calculations are performed with HSC Chemistry and MATLAB. The main focus of this investigation is a low temperature methanation (300 °C) at ambient pressure. These parameter settings result from the current efforts in the design and construction of a lab-scale fluidized bed methanation test rig at TU Wien for the given parameters. Nevertheless, also a temperature variation from 200 °C to 500 °C and a pressure range from 1 bar_a to 10 bar_a are carried out. Graphite is chosen as the prevailing carbon species, since Frick et al. [19] found that the Gibbs free energy is lower than for amorphous carbon and is thus preferentially formed.

In order to classify the feed gas composition the stoichiometric number (SN) is defined.

$$SN = \frac{y_{H_2}}{3*y_{CO}+4*y_{CO_2}+2*y_{C_2H_4}} \quad (8)$$

SN gives the ratio between the molar fraction of H_2 (y_{H_2}) to the molar fractions of the carbonaceous species in the feed gas which react to CH_4. If SN is equal to one, there is a stoichiometric amount of H_2 available according to Eqs. 1, 3 and 4. Because the regarded pressures in this study are relatively low, it is safe to assume ideal gas behavior. Molar fraction are thus equal to volume fractions. This definition of SN is not unambiguous, because the chemical equilibrium is influenced by all available species and therefore also by CH_4 and H_2O. Nevertheless, it allows an approximate classification of the feed gas mixture. Typical product gases from the DFB gasification show similar CH_4 concentrations. Water concentrations in the feed gases are assumed zero. This is attributed to the required gas cleaning which is conventionally carried out at low temperatures [21]. If similar CH_4 concentrations and a water free feed gas are assumed, the implementation of SN is justified.

Additionally, the CH_4 yield (Y_{CH_4}),

$$Y_{CH_4} = \frac{\dot{n}_{CH_4,eq}}{\sum_i N_i \dot{n}_{i,feed}} * 100 \quad (9)$$

the carbon yield (Y_C),

$$Y_C = \frac{\dot{n}_{C,eq}}{\sum_i N_i \dot{n}_{i,feed}} * 100 \quad (10)$$

the CO conversion (X_{CO}), and

$$X_{CO} = \frac{\dot{n}_{CO,feed} - \dot{n}_{CO,eq}}{\dot{n}_{CO,feed}} * 100 \quad (11)$$

the CO_2 conversion (X_{CO_2}) are defined.

$$X_{CO_2} = \frac{\dot{n}_{CO_2,feed} - \dot{n}_{CO_2,eq}}{\dot{n}_{CO_2,feed}} * 100 \quad (11)$$

Index i refers to the carbonaceous species in the feed ($i = CH_4, CO, CO_2, C_2H_4$).

Gas cleaning is not within the scope of this study. The feed gas mixture for the methanation is assumed free of impurities and other minor components. Besides, kinetics or heat and mass transfer phenomena are not considered.

Tab. 1: Investigated feed gases

Parameter	Unit	Feed gas number					
		1	2	3	4	5	6
Source	-	[5]	[3]	[22]	[23]	[24]	[25]
Gasification agent	-	H_2O	H_2O	H_2O	H_2O	CO_2/H_2O[a]	H_2O
Feedstock	-	BA	BA	LI	SS	RSC	SW
Bed material	-	L	L	O	O/L[b]	O	L
Gasification temperature	°C	625	761	789	800	840	582-797
Combustion temperature	°C	820	998	945	945	938	830-1041
Feed gas composition (water free feed)							
H_2	vol.-%	68.3	52.4	42.6	35.6	25.8	71.1-47.6
CO	vol.-%	6.5	18.4	21.2	13.7	32.1	7.3-21.6
CO_2	vol.-%	8.9	21.3	21.8	36.5	33.7	4.1-23
CH_4	vol.-%	14.5	7.3	12.0	11.7	7.3	17.4-8.8
C_2H_4	vol.-%	1.9	0.6	2.4	2.5	1.1	1.9-0.5

[a] CO_2/H_2O = 68/32 vol.-%
[b] O/L = 80/20 wt.-%

3. Results and discussion

In Tab. 1 the investigated feed gas compositions for the methanation are shown. Feed gas no. **1** shows a typical SER gas with high hydrogen content. Limestone (L) is used as bed material at lower temperatures and bark (BA) is chosen as the feedstock. Feed gases no. **2**-no. **4** present product gases from conventional gasification. With feed gas no. **2** the same fuel and bed material is used but the gasification temperature is higher which results in lower H_2 and higher CO and CO_2 contents. For feed gas no. **3** lignin (LI) is used as fuel and olivine (O) as bed material. Sewage sludge (SS) and an olivine/limestone mixture (O/L) are the basis for feed gas no. **4**, which results in low H_2 and high CO_2 contents. For feed gas no. **5**, a CO_2/H_2O mixture is used as gasification agent and rapeseed cake (RSC) and O as fuel and bed materials, respectively. This results in even lower H_2 and high CO and CO_2 concentrations. Feed gas no. **6** shows a temperature variation for SER gasification. This is included to demonstrate the adaptability of the DFB gasifier to the requirements of the methanation process (also see Fig. 4). Data for this variation is only available for softwood (SW) as feedstock.

In Fig. 1 results of chemical equilibrium calculations at 300 °C and 1 bar_a are shown for feed gas nos. **1-5**. The volume fractions of the dry gas components after methanation (referred to as raw-SNG) and the water content of the raw-SNG are depicted. C_2H_4 is not displayed in any of the figures, because it is completely converted under all investigated conditions. CO is not shown in Fig. 1, because only trace amounts remain in the raw-SNG. Additionally, Tab. 2 lists some key figures as defined in Eqs. 8-11.

Almost complete conversion of CO and CO_2 to CH_4 can be reached with the SER feed gas (feed gas no. **1**). The CH_4 yield is

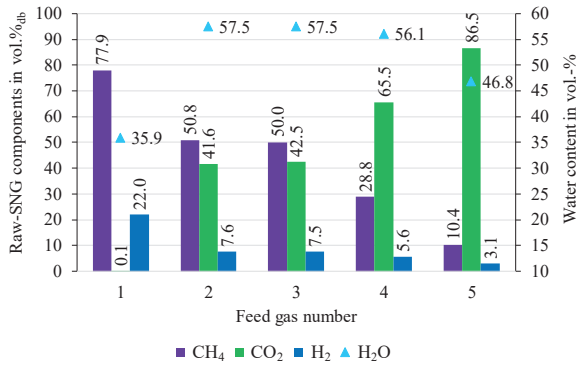

Fig. 1: Raw-SNG gas composition for feed gas nos. 1-5 at 1 bar_a and 300 °C

Tab. 2: Key figure results of the equilibrium calculations

Par.	Unit	Feed gas number				
		1	2	3	4	5
SN	-	1.16	0.37	0.27	0.19	0.11
Y_{CH_4}	%	99.9	29.4	24.6	14.4	5.2
Y_C	%	0	46.5	54.5	52.8	50.9
X_{CO}	%	100	99.9	99.9	99.8	99.9
X_{CO_2}	%	99.7	45.4	42.7	39.9	2.2

99.9 % and no carbon formation is thermodynamically expected. However, 22 vol.-$\%_{db}$ of H_2 are still in the raw-SNG and would have to be separated before grid feed-in below 4 vol.-%. Feed gas nos. **2** and **3** show similar results to each other. About 50 vol-$\%_{db}$ CH_4 can be expected. CO is almost completely transformed, whereas less than 50% of the CO_2 is converted. Thermodynamically, severe carbon deposition can occur with about half of the feed carbon being separated from the gas stream. The raw-SNG from the SS product gas (feed gas no. **4**) shows a CH_4 yield of only 14.4 %. The rest of the gas is mainly CO_2. If a product gas from CO_2 gasification is used (feed gas no. **5**), 86.5 vol.-$\%_{db}$ of the raw-SNG consists of CO_2 and only 10.4 vol.-$\%_{db}$ are CH_4. This is equal to a methane yield of 5.2 % and a CO_2 conversion of 2.2%, respectively.

For feed gas nos. **2-5** the SN is below one. Since all feed gases are dry, this correlates with the carbon deposition. CO is almost completely converted for all feed gases. However, even small amounts of CO might exceed the allowed threshold level for grid feed-in on the one hand. On the other hand, CO_2 methanation is found to be kinetically hindered even for very low CO concentrations [26]. For feed gas no. **1** 7 $ppm_{v,db}$ of CO remain in the raw-SNG in the thermodynamic equilibrium. At least 580-750 $ppm_{v,db}$ need to be expected for feed gas nos. **2-5**.

Investigation of the sewage sludge product gas

In the following section a more in-depth discussion of the SS product gas follows (feed gas no. **4**). Because of the expected carbon deposition for this feed gas composition, H_2O should be added if a long catalyst lifetime and a high conversion efficiency are aimed at. Fig. 2 depicts the raw-SNG gas composition after the addition of H_2O for temperatures from 200-500 °C and pressures of 1, 5 and 10 bar_a (Fig. 2b). The amount of water added corresponds to the minimum amount needed to prevent carbon deposition. This minimum volume fraction of H_2O in the feed gas (H_2O_{feed}) as well as Y_{CH_4} are also displayed (Fig. 2a). With increasing temperature, less CH_4 and CO_2 and more CO and H_2 are present. Accordingly, the CH_4 yield decreases from 41 % to 26 % with increasing temperature

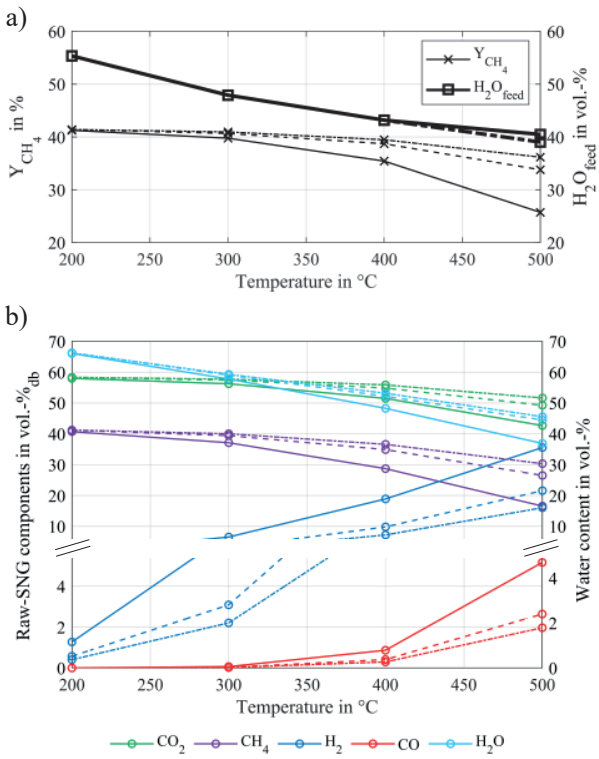

Fig. 2: Temperature and pressure variation for feed gas no. 4 in the thermodynamic equilibrium: 1 bar_a (full line), 5 bar_a (dashed line) and 10 bar_a (dash-dotted line). a) CH_4 yield and feed water content, b) Raw-SNG gas composition

at 1 bar_a. H_2O_{feed} decreases from 55 vol.-% to 40 vol.-% within the displayed temperature range. Nevertheless, the methanation would be preferred at low temperatures from a thermodynamic point of view, if the additionally required steam is not seen as the decisive factor. Especially the strongly rising CO content at higher temperatures makes low temperature methanation attractive. Pressure only has a significant influence on the gas composition at higher temperatures. At 500 °C Y_{CH_4} can be substantially elevated if the pressure is increased to 5 bar_a. A further pressurization only allows a minor improvement of Y_{CH_4}. Whereas, at 200 °C Y_{CH_4} is almost constant for all pressures. For H_2O_{feed}, hardly any influence of pressure can be observed.

A comparison of Fig. 1 and Fig. 2 clarifies the influence of the added feed water at 300 °C and 1 bar_a for the SS product gas. By the addition, the CH_4 content is elevated from 29 to 37 vol.-$\%_{db}$. At the same time, the CO_2 content is lowered from 66 to 56 vol.-$\%_{db}$. H_2 slightly increases from 5.6 to 6.6 vol.-%. The CO concentration is marginally lowered from 714 to 667 $ppm_{v,db}$. Despite the addition of 48 vol.-% of H_2O to the dry feed gas, the H_2O concentration in the raw-SNG only increases slightly. This can be visualized by the steam gasification reaction (Eq. 7). Most of the steam is needed to gasify the carbon. Because no carbon is present after feed water addition, X_{CO_2} is negative under all displayed conditions. In other words, more CO_2 is formed during methanation than converted.

For grid feed-in the raw-SNG needs to be freed of CO_2. A maximum of only 2 vol.-% is allowed. A H_2 content below the allowed threshold level of 4 vol.-% after CO_2 separation could be achieved by increasing the pressure at 260 °C to 10 bar_a. If the desired commodity is hythane only CO_2 separation is necessary.

Investigation of the SER product gas

Feed gas no. **1** is a typical SER product gas with a high H_2 content. SN is greater than one, which allows a practically complete methanation of the carbon oxides ($CO+CO_2$) at temperatures below 300 °C with a CH_4 yield of nearly 100 % (Fig. 3). Pressure again only has significant influence on the gas composition at higher temperatures. With pressurization, the decreasing trend of CH_4 and the increasing trends of H_2, CO and CO_2 at higher temperatures can be counteracted. In addition, above 440 °C at 1 bar_a carbon formation is thermodynamically possible. As is shown in Fig. 3a, H_2O needs to be added. At higher pressures, this can be prevented. Below 300 °C there is practically no influence of pressure or temperature on the gas composition.

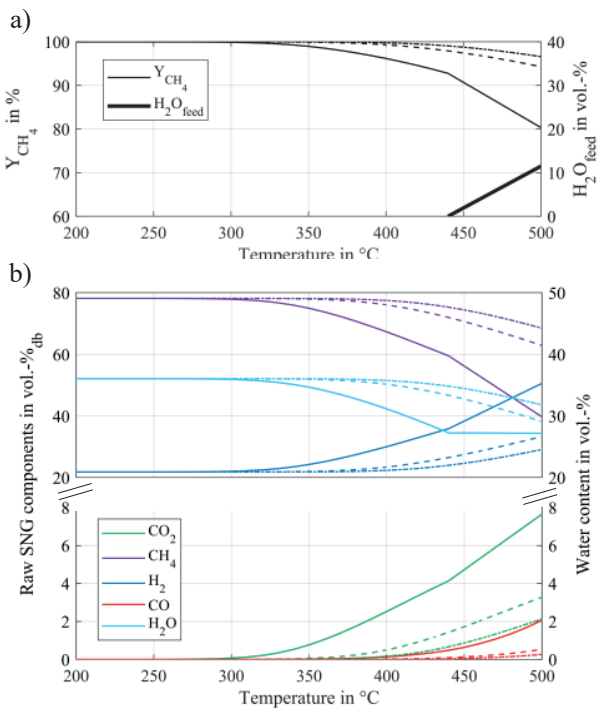

Fig. 3: Temperature and pressure variation for feed gas no. 1 in the thermodynamic equilibrium: 1 bar_a (full line), 5 bar_a (dashed line) and 10 bar_a (dash-dotted line). a) CH_4 yield, b) Raw-SNG gas composition

Methanation around 300 °C and 1 bar_a shows a favorable raw-SNG composition without the need of compression. Lower temperatures would not improve the gas composition, but increase the challenge of employing an active catalyst. For grid feed-in, only H_2 would need to be separated from the raw-SNG. For the application as hythane on the other hand, no further upgrading step is necessary except water condensation.
Besides these advantages, the methanation of SER product gas also comes with drawbacks. The high H_2 content can only be reached by the increased transport of carbon from the fuel to the flue gas. However, the excess carbon (in the form of CO_2), which is still in the raw-SNG in case of conventional gasification, is already removed within the gasification process for the SER product gas. The overall process chain thus shows a low carbon utilization factor. But this lower carbon utilization factor lies primarily in the gasification process and not in the methanation process. Whereas the addition of H_2 from external sources (e.g. electrolysis) would allow the methanation of the leftover CO_2 and yield a high carbon utilization factor for conventional gasification. Another suggestion would be the installation of a water gas shift reactor prior to the methanation reactor, which was demonstrated successfully for hydrogen production from DFB derived wood gas [27].

Investigation of variable product gas compositions of the SER process

Fuchs et al. [25] already described the adaptability of the SER process with regard to the product gas composition. In Fig. 4 the evolution of the product gas components over the gasification temperature of the 100 kW_{th} DFB gasifier at TU Wien is depicted. By temperature variation, the product gas can be adjusted

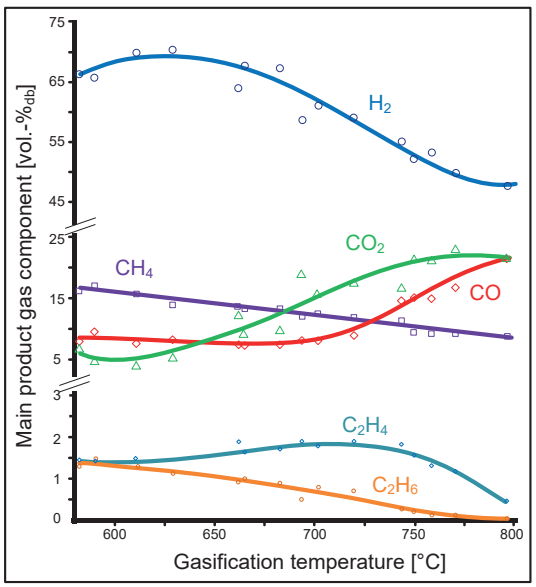

Fig. 4: Product gas composition over gasification temperature for the 100 kW_{th} DFB gasifier at TU Wien for softwood and olivine as fuel and bed material, respectively; from [25]

to the required feed gas for methanation. However, this also adds an additional parameter to the modelling of the methanation reactions.
Fig. 5 displays the composition of the raw-SNG in the thermodynamic equilibrium for all data points of Fig. 4 over SN. Temperature and pressure are again set to 300 °C and 1 bar_a for the methanation process, respectively. In order to assess carbon formation Y_C is given. There is a decreasing trend for CO_2, H_2O and the amount of carbon formed for an increasing SN. CH_4 has a maximum at a SN slightly above one. At the same point carbon formation declines to zero and the small incline in H_2 turns into a sharp increase for higher SN. CO is only present in trace amounts (0.14-614 $ppm_{v,db}$) and is not displayed here. From a thermodynamic point of view, the feed gas with a SN of 1.09 generates a raw-SNG with the most favorable composition for the methanation at 300 °C and 1 bar_a. A SN of 1.09 corresponds to a gasification temperature of about 680 °C.

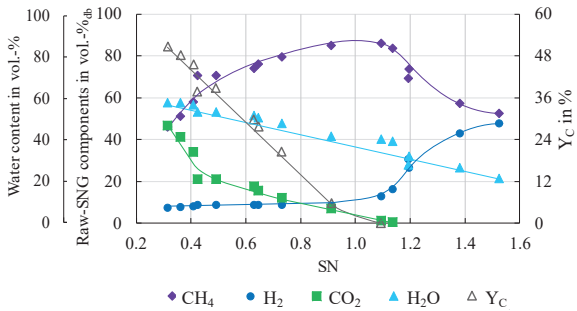

Fig. 5: Raw-SNG gas composition and Y_C over SN for the feed gas compositions according to Fig. 4 at 300 °C and 1 bar_a in the thermodynamic equilibrium

The associated compositions for the feed gas and the raw-SNG as well as the key figures are depicted in Tab. 3. Different operation conditions of the methanation might favor other feed gas compositions from Fig. 4 and vice versa. In order to find the most suitable feed gas composition for deviating methanation conditions, reiterations of the thermodynamic equilibrium calculations would have to be carried out.

Tab. 3: Feed gas and raw-SNG composition and key figures for the feed gas with a SN of 1.09 at 300 °C and 1 bar_a in the thermodynamic equilibrium

Par.	Unit	Feed gas	Raw-SNG
CH_4	vol.-$\%_{db}$	13.3	86.1
H_2	vol.-$\%_{db}$	67.8	12.8
CO	vol.-$\%_{db}$	7.3	0.005
CO_2	vol.-$\%_{db}$	9.8	1.1
C_2H_4	vol.-$\%_{db}$	1.7	0
H_2O	vol.-%	0	40.2
Y_{CH_4}	%	98.8	
Y_C	%	0	
X_{CO}	%	100	
X_{CO_2}	%	95.8	

4. Conclusion and Outlook

In this work, the suitability of various product gases from the 100 kW_{th} DFB gasifier for methanation has been evaluated from a thermodynamic point of view. It has been shown, that complete methanation is only possible for SER product gases. For all other gases, only the partial methanation of CO is possible, whereas CO_2 might even constitute the main raw-SNG component. Additionally, gases from conventional steam gasification or gasification with CO_2 admixture to the gasification agent (H_2O+CO_2) are subject to carbon deposition. Therefore, H_2O needs to be added for a stable operation. Furthermore, the influence of different operation conditions of the methanation on the raw-SNG composition have been visualized. By the careful choice of operation conditions, energy savings and/or less effort for further gas upgrading can be accomplished. A further investigation of the SER product gases has revealed that it is also possible to adapt the gasification process to suit certain methanation conditions optimally. However, if H_2 is available from an external source, conventional gasification can be beneficial because of a higher carbon utilization factor.

It should be noted that all investigations in this paper are based on thermodynamic equilibrium calculations. There are many other parameters, which can influence the performance of the methanation. Catalyst poisoning due to insufficient gas cleaning, the choice of the reactor concept or kinetic limitations necessitate experimental investigations.

Acronyms

BA	bark
DFB	dual fluidized bed
L	limestone
LI	lignin
O	olivine
O/L	olivine/limestone mixture
raw-SNG	synthetic natural gas after methanation/before gas upgrading
RSC	rapeseed cake
SER	sorption enhanced reforming
SNG	synthetic natural gas
SS	sewage sludge

SW	softwood
vol.-%	volumetric percent
wt.-%	weight percent

Symbols

ΔH_R^{300}	molar reaction enthalpy at 300 °C
H_2O_{feed}	volume fraction of H_2O in the feed in vol.-%
$\dot{n}_i$	molar flow of species i in mol/s
N_i	number of carbon atoms in species i
SN	stoichiometric number
X_{CO}	carbon monoxide conversion in %
X_{CO_2}	carbon dioxide conversion in %
Y_C	carbon yield in %
Y_{CH_4}	methane yield in %
y_i	molar fraction of species i

Indices

a	absolute
C	carbon
CH_4	methane
C_2H_4	ethylene
CO	carbon monoxide
CO_2	carbon dioxide
db	dry basis
eq	equilibrium
feed	in the feed gas
H_2	hydrogen
v	volumetric

5. Acknowledgements

This work is part of the research project ReGas4Industry and receives financial support from the research program “Energieforschung” funded by the Austrian Climate and Energy Fund.

6. References

[1] European Commission, “Directive (EU) 2018/2001 of the European Parliament and of the Council of 11 December 2018 on the promotion of the use of energy from renewable sources,” *Off. J. Eur. Union*, vol. L 328/82, no. December, p. 128, 2018.

[2] I. E. A. (IEA), *Gas market report 2O18*. 2018.

[3] F. Benedikt, J. C. Schmid, J. Fuchs, A. M. Mauerhofer, S. Müller, and H. Hofbauer, “Fuel flexible gasification with an advanced 100 kW dual fluidized bed steam gasification pilot plant,” *Energy*, vol. 164, pp. 329–343, 2018.

[4] A. Sahoo and D. K. Ram, “Gasifier performance and energy analysis for fluidized bed gasification of sugarcane bagasse,” *Energy*, vol. 90, pp. 1420–1425, 2015.

[5] J. Fuchs, J. C. Schmid, S. Müller, and H. Hofbauer, “Dual fluidized bed gasification of biomass with selective carbon dioxide removal and limestone as bed material: A review,” *Renew. Sustain. Energy Rev.*, vol. 107, no. November 2018, pp. 212–231, 2019.

[6] M. Asadullah, “Biomass gasification gas cleaning for downstream applications : A comparative critical review,” vol. 40, pp. 118–132, 2014.

[7] T. Pröll, I. G. Siefert, A. Friedl, and H. Hofbauer, “ Removal of NH_3 from Biomass Gasification Producer Gas by Water Condensing in an Organic Solvent Scrubber,” *Ind. Eng. Chem. Res.*, vol. 44, no. 5, pp. 1576–1584, 2005.

[8] H. Hofbauer, R. Rauch, S. Fürnsinn, and C. Aichernig, “Energiezentrale Güssing,” 2006.

[9] J. Kopyscinski, T. J. Schildhauer, and S. M. A. Biollaz, “Production of synthetic natural gas (SNG) from coal and dry biomass - A technology review from 1950 to 2009,” *Fuel*, vol. 89, no. 8, pp. 1763–1783, 2010.

[10] T. J. Schildhauer and S. M. A. Biollaz, *Synthetic Natural Gas from Coal, Dry Biomass, and Power-to-Gas Applications*. 2016.

[11] ÖVGW, *Richtlinie G 31-Erdgas in Österreich-Gasbeschaffenheit*. 2001.

[12] M. Kraussler, P. Schindler, and H. Hofbauer, “An experimental approach aiming the production of a gas mixture composed of hydrogen and methane from biomass as natural gas substitute in industrial applications,” *Bioresour. Technol.*, vol. 237, no. 2017, pp. 39–46, 2017.

[13] F. Benedikt, M. Kuba, J. Christian, S. Müller, and H. Hofbauer, “Assessment of correlations between tar and product gas composition in dual fluidized bed steam gasification for online tar prediction,” *Appl. Energy*, vol. 238, no. December 2018, pp. 1138–1149, 2020.

[14] X. Bai, S. Wang, T. Sun, and S. Wang, “Influence of Operating Conditions on Carbon Deposition Over a Ni Catalyst for the Production of Synthetic Natural Gas (SNG) from Coal,” pp. 2157–2166, 2014.

[15] A. Kambolis, T. J. Schildhauer, and O. Kröcher, “CO Methanation for Synthetic Natural Gas Production,” vol. 69, no. 10, pp. 608–613, 2015.

[16] S. Rönsch, J. Schneider, S. Matthischke, M. Schlüter, M. Götz, J. Lefebvre, P. Prabhakaran and S. Bajohr, Review on methanation – From fundamentals to current projects,” *Fuel*, vol. 166, pp. 276–296, 2016.

[17] J. Kopyscinski, T. J. Schildhauer, and S. M. A. Biollaz, “Methanation in a fluidized bed reactor with high initial CO partial pressure : Part II — Modeling and sensitivity study,” *Chem. Eng. Sci.*, vol. 66, no. 8, pp. 1612–1621, 2011.

[18] J. Kopyscinski, T. J. Schildhauer, F. Vogel, S. M. A. Biollaz and A. Wokaun, “Applying spatially resolved concentration and temperature measurements in a catalytic plate reactor for the kinetic study of CO methanation,” *J. Catal.*, vol. 271, no. 2, pp. 262–279, 2010.

[19] V. Frick, J. Brellochs, and M. Specht, “Application of ternary diagrams in the design of methanation systems,” vol. 118, pp. 156–160, 2014.

[20] J. Gao, Y. Wang, Y. Ping, D. Hu, G. Xu, and F. Su, “RSC Advances PAPER: A thermodynamic analysis of methanation reactions of carbon oxides for the production of synthetic natural gas,” pp. 2358–2368, 2012.

[21] N. Abdoulmoumine, S. Adhikari, A. Kulkarni, and S. Chattanathan, “A review on biomass gasification syngas cleanup,” *Appl. Energy*, vol. 155, pp. 294–307, 2015.

[22] J. C. Schmid, F. Benedikt, J. Fuchs, A. M. Mauerhofer, S. Müller, and H. Hofbauer, “Syngas for biorefineries from thermochemical gasification of lignocellulosic fuels and residues - 5 years’ experience with an advanced dual fluidized bed gasifier design,” *Biomass Convers. Biorefinery*, 2019.

[23] J. C. Schmid, A. Bartik, F. Benedikt, A.M. Mauerhofer, J. Fuchs, E. Schanz, S. Reisinger, B. Nowak, F. Bühler, M. Österreicher, A. Lunzer, C. Walcher, S. Müller, M. Fuchs and H. Hofbauer, “Steam gasification of sewage sludge for synthesis processes,” in *ICPS 2019*, 2019.

[24] A. M. Mauerhofer, S. Müller, F. Benedikt, J. Fuchs, A. Bartik, and H. Hofbauer, “CO_2 Gasification of Biogenic Fuels in a Dual Fluidized Bed Reactor System,” *Submitt. to Biomass Convers. Biorefinery*, 2019.

[25] J. Fuchs, J. C. Schmid, S. Müller, A. M. Mauerhofer, F. Benedikt, and H. Hofbauer, "The impact of gasification temperature on the process characteristics of sorption-enhanced reforming of biomass," *Biomass Convers. Biorefinery*, 2019.

[26] T. Herwijnen, H. Doesburg, and W. A. de Jong, "Kinetics of the Methanation of CO and CO_2 on a Nickel Catalyst," *J. Catal.*, vol. 28, pp. 391–402, 1973.

[27] S. Fail, N. Diaz, F. Benedikt, M. Kraussler, J. Hinteregger, K. Bosch, M. Hackel, R. Rauch and H. Hofbauer, "Wood gas processing to generate pure hydrogen suitable for PEM fuel cells," *ACS Sustain. Chem. Eng.*, vol. 2, no. 12, pp. 2690–2698, 2014.